Vibrational Circular Dichroism in Amino Acids and Peptides. 6. Localized Molecular Orbital Calculations of the Carbon-Hydrogen Stretching Vibrational Circular Dichroism in Deuterated Isotopomers of Alanine

Teresa B. Freedman,[1a] Max Diem,[1b] Prasad L. Polavarapu,[1c] and Laurence A. Nafie*[1a,d]

Contribution from the Departments of Chemistry, Syracuse University, Syracuse, New York 13210, City University of New York, Hunter College, New York, New York 10021, and Vanderbilt University, Nashville, Tennessee 37235.
Received August 14, 1981

Abstract: Results of localized molecular orbital (LMO) calculations of vibrational circular dichroism (VCD) for alanine-N-d_3, alanine-C^*-d_1-N-d_3 and alanine-C-d_3-N-d_3 are presented and found to be in close agreement with experiment for the signs and relative intensities of the eight fundamental CH stretching vibrations in these molecules. Spectral simulations of the LMO-VCD and absorption intensities are presented and compared with the experimental spectra. Stereoprojections of the eight vibrational modes in these alanine molecules are provided which show the relative magnitude and direction of the displacements of the nuclei and the LMO centroids. The results are analyzed in terms of these displacements, and conclusions regarding the importance of vibrationally induced electronic motion in the calculated VCD are discussed. These calculations provide a basis for further theoretical studies of VCD in alanine and related molecules as well as other simple chiral molecules for which VCD is available. The LMO approach appears to be particularly valuable in those cases where electronic motion as distinct from the nuclear motion is important and where consequently the usual fixed partial charge model is inadequate.

In the preceding two papers[2,3] we first established vibrational assignments and a consistent Urey-Bradley force field for various deuterium isotopomers of alanine and then focused our attention on the vibrational circular dichrosim (VCD) in the CH stretching vibrations, analyzing this region in greater detail, developing a more accurate force-field description, and finally carrying out fixed partial charge (FPC)[4] calculations of intensities. In the present paper we extend our analysis by carrying out localized molecular orbital (LMO)[5] calculations of the VCD and absorption intensities for the CH stretching spectra in these molecules. Only two previous investigations of LMO-VCD calculations have been carried out to date,[6,7] and hence the method is still rather unexplored. In these initial LMO-VCD studies the two molecules, neopentyl-*1-d* chloride[6] and (+)-3-methylcyclohexanone,[7] were chosen on the basis of having accurate force fields available and showing close agreement between FPC calculations and experiment. The LMO-VCD results for these molecules were found to be as accurate as the corresponding FPC results.

The present LMO calculations are deserving of special interest since here the agreement between FPC calculations and experiment for alanine, particularly the CH deuterated species, is less than favorable. In fact, our motivation for moving ahead with the LMO-VCD calculations at this time was in search of an explanation of the large gap between calculated and observed VCD intensities in two of the four fundamental CH modes of alanine-N-d_3 and all the CH modes in alanine-C^*-d_1-N-d_3 and alanine-C-d_3-N-d_3. We discovered that the LMO-VCD results for our best force field predicts the correct sign and gives close relative magnitudes for *all eight* vibrations for which we have VCD data. An interesting question of absolute magnitude still remains which we will address below, but we now have confidence in our vibrational force field and the resulting displacements of the nuclei for the individual CH stretching modes.

In addition to presenting calculated LMO rotational and dipole strengths we provide spectral simulations using predetermined bandwidths and positions for direct comaprison to the experimental spectra. The visual aspects of these calculations are also shown as stereoprojections of alanine for each normal mode where the equilibrium structure and the relative displacements of the nuclei and the LMO centroids can be seen. This is particularly useful in viewing the degree to which the centroid displacements follow the vibrational nuclear displacements. These diagrams contain a richness of electronic information which is not present in FPC calculations. Specifically, it is the departure of the electronic motion, as described by the LMO centroids, from perfect nuclear following which reveals information regarding the coupling of the centroid motions among themselves as well as to the nuclear motion.

Experimental Section

The localized molecular orbital calculations were carried out using CNDO/2 molecular orbital wave functions[8,9] which were subsequently localized using the criteria of Edmiston and Ruedenberg.[10,11] The determination of the orbital centroids, their displacements, and the procedure used to calculate VCD and absorption intensities have been described previously.[6,7] All of the intensity calculations were carried out at Syracuse University using a Dec-10 computer system.

Spectral simulations were performed using the Nicolet 1180E data system associated with the Nicolet 7199 Fourier transform spectrometer at Syracuse. The Nicolet curve analysis program (CAP) allowed us to synthesize absorption and VCD spectra using bandwidths and positions deduced from the spectral decomposition of the experimental absorption spectra as described in the previous paper[3] and having integrated intensities associated with the LMO rotational and dipole strength calculated in the present paper.

The stereoprojections of L-alanine showing the nuclear and centroid vibrational displacements were drawn using a modified ORTEP program at Vanderbilt University.

Methodology

Since only two applications of the LMO model to VCD have appeared in the literature,[6,7] and then only recently, we briefly describe the basic equations and procedures used to calculate the

(1) (a) Syracuse University. (b) City University of New York. (c) Vanderbilt Universlty. (d) Alfred P. Sloan Foundation Fellow, 1978-1982.
(2) Diem, M.; Polavarapu, P. L.; Oboodi, M.; Nafie, L. A. *J. Am. Chem. Soc.*, first of two preceding papers in this issue.
(3) Lal, B. B.; Diem, M.; Polavarapu, P. L.; Oboodi, M.; Freedman, T. B.; Nafie, L. A. *J. Am. Chem. Soc.*, preceding paper in this issue.
(4) Schellman, J. A. *J. Chem. Phys.* **1973**, *58*, 2882; **1974**, *60*, 343.
(5) Nafie, L. A.; Walnut, T. H. *Chem. Phys. Lett.* **1977**, *49*, 441. Walnut, T. H.; Nafie, L. A. *J. Chem. Phys.* **1977**, *67*, 1491; **1977**, *67*, 1501.
(6) Nafie, L. A.; Polavarapu, P. L. *J. Chem. Phys.* **1981**, *75*, 2935.
(7) Polavarapu, P. L.; Nafie, L. A. *J. Chem. Phys.* **1981**, *75*, 2945.
(8) Pople, J. A.; Santry, D. P.; Segal, G. A. *J. Chem. Phys.* **1965**, *43*, 5130. Pople, J. A.; Beveridge, D. L. "Approximate Molecular Orbital Theory"; McGraw-Hill: New York, 1971.
(9) Dobish, P. A. *QCPE* **1969**, *11*, 141.
(10) Edmiston, C.; Ruedenberg, K. *Rev. Mod. Phys.* **1963**, *35*, 457.
(11) Hunter, J. A. *QCPC* **1978**, *11*, 355.

0002-7863/82/1504-3343$01.25/0

rotational strengths and dipole strengths with this model. Within the harmonic oscillator approximation, the dipole strength for the transition between the zeroth and first level of the αth normal mode can be written as[5-7]

$$D^{\alpha}_{10} = \frac{e^2\hbar}{2\omega_\alpha}[\sum_n Z_n \mathbf{s}_{n\alpha} - \sum_k \sigma_{k\alpha}]^2 \quad (1)$$

where e is the quantum of electric charge, $\hbar$ is planck's constant divided by 2π, ω_α is the radial frequency of the vibrational transition, Z_n is the charge of the nth nucleus, $\mathbf{s}_{n\alpha}$ is the vector representing the derivative of the position of the nth nucleus with respect to displacement along the αth normal mode, and $\sigma_{k\alpha}$ is the corresponding derivative of the position of the centroid of the kth molecular orbital. Under these same conditions the rotational strength, which is a measure of the VCD intensity, is given by eq 2, where $\mathbf{R}_{n,0}$ and $\mathbf{r}_{k,0}$ are the equilibrium positions of the nth

$$R^{\alpha}_{10} = \frac{e^2\hbar}{4c}[\sum_{n>n'} Z_n Z_{n'}(\mathbf{R}_{n,0}-\mathbf{R}_{n',0})\cdot\mathbf{s}_{n\alpha} \times \mathbf{s}_{n\alpha'} + \sum_{k>k'}(\mathbf{r}_{k,0} - \mathbf{r}_{k',0})\cdot \sigma_{k\alpha} \times \sigma_{k'\alpha} - \sum_{n,k} Z_n(\mathbf{R}_{n,0} - \mathbf{r}_{k,0})\cdot\mathbf{s}_{n\alpha} \times \sigma_{k\alpha}] \quad (2)$$

nucleus and kth molecular orbital centroid, respectively. Equation 1 is simply the square of the electric transition moment and is invariant with respect to localization of the molecular orbitals; it is a standard expression for the calculation of infrared intensities using molecular orbitals. Equation 2, on the other hand, is the imaginary part of the vector dot product of the electric transition moment with the LMO magnetic transition moment and depends heavily upon localization of the molecular orbitals. Localization ensures that the rotational strength will be represented well by the motions of the nuclei and orbital centroids with respect to one another and that intrinsic rotational strength contributions arising from the vibrational rocking motions of individual orbitals about their centroid position will be small.[5,6]

In order to calculate R^{α}_{10} and D^{α}_{10}, we first determine the equilibrium molecular structure which is specified by the vector set, $\mathbf{R}_{n,0}$. In addition, the nuclear displacement vectors, $\mathbf{s}_{n\alpha}$, are needed and can be obtained by a normal coordinate analysis. We next determine the equilibrium location of localized orbital centroids $\mathbf{r}_{k,0}$ and then by displacing the nuclei along the individual normal coordinates we calculate the vectors $\sigma_{k\alpha}$ by obtaining finite difference derivatives from the displaced centroid positions relative to their equilibrium positions.

Results

In Table I we present the results of two sets of LMO calculations of dipole and rotational strength and their comparison to experiment. The experimental values are the same as those listed in the previous paper where the results of FPC calculations were presented.[3] The first LMO calculation (I) corresponds to a Urey–Bradley force field which takes into account the Fermi resonance interaction of the methyl deformation overtones with the symmetric methyl stretching frequency but which retains a symmetric force-field description of the methyl group and hence has very little splitting in the antisymmetric methyl stretching frequencies. The second LMO calculation (II) then introduces splitting in the antisymmetric modes in addition to the Fermi resonance modification. With the exception of a minor difference in the methyne C*–H stretching mode in calculation I, both of these force fields are unchanged from those previously described.[3]

In comparing these two LMO calculations we note that only a mild increase in rotational strength intensity is registered in calculation II for alanine-N-d_3 and -C^*-d_1-N-d_3, whereas a rather large increase in intensity occurred in the FPC calculation upon lifting the force-field symmetry of the methyl group.[3] Second, there is a difference in sign of the antisymmetric methyl couplet in alanine-C^*-d_1-N-d_3 for the two calculations. The correct sign pattern appears in calculation II when the methyl frequencies are split in a manner which preserves the pattern of relative nuclear motions of these two modes as they arise in alanine-N-d_3 for calculation I. The motions are not maintained in alanine-C^*-d_1-N-d_3 in calculation I; here they are heavily mixed from the pure

Table I. Results of LMO Calculations of Rotational and Dipole Strength for Alanine and Its Deuterated Isotopomers in the CH Stretching Region

molecule	experiment[a]				LMO calculation I[b]				LMO calculation II[c]			
	frequency (cm^{-1})	$R \times 10^{44}$ ($esu^2\ cm^2$)	$D \times 10^{39}$ ($esu^2\ cm^2$)	$g \times 10^5$	frequency (cm^{-1})	$R \times 10^{44}$ ($esu^2\ cm^2$)	$D \times 10^{39}$ ($esu^2\ cm^2$)	$g \times 10^5$	frequency (cm^{-1})	$R \times 10^{44}$ ($esu^2\ cm^2$)	$D \times 10^{39}$ ($esu^2\ cm^2$)	$g \times 10^5$
L-Ala-N-d_3	3009	0.54	0.57	3.79	3000	1.53	2.45	2.50	3007	1.77	2.21	3.20
	2989	−2.43	0.58	−16.75	2999	−5.14	5.56	−3.70	2993	−9.06	5.13	−7.06
	2970	5.58	0.45	49.60	2963	13.98	5.13	10.90	2970	18.56	4.80	15.47
	2949	−0.75	0.34	−8.82	2950	−4.62[d]	1.19[d]	−15.57[d]	2950	−5.20[d]	2.03[d]	−10.24[d]
	2915		0.10									
	2892		0.20									
L-Ala-C^*-d_1-N-d_3	3008	−0.40	0.20	−8.00	2894	−1.92	0.49	−15.67	2892	−2.15	0.841	−10.24
	2987	0.70	0.53	5.28	2999	−0.736	1.75	1.69	3007	0.945	1.45	2.61
	2948	−0.53	0.67	−3.16	2998	0.781	5.40	0.579	2992	−0.372	4.72	−0.315
	2912	−0.31	0.36	−3.44	2951	−0.491[d]	1.49[d]	−1.32[d]	2951	−0.870[d]	2.23[d]	−1.56[d]
	2891		0.03									
L-Ala-C-d_3-N-d_3	3015	−0.08	0.16	−2.00	2893	−0.203	0.618	−1.32	2893	−0.360	0.923	−1.56
	2968		0.39									
	2944	2.11	0.37	22.81	2962	4.59	5.75	3.19	2970	4.58	5.74	3.19
	2894		0.04									
			0.02									

[a] Estimates of integrated band intensities based on curve resolutions of the experimental data which yielded band-center frequencies and half-widths. [b] Unsplit methyl force-field[3] calculation including Fermi resonance interaction. The C*–H stretching force constant is 4.09 instead of 4.101 as reported in the previous paper; all other force constants were unchanged. [c] Split methyl force-field calculation including Fermi resonance interaction. [d] 29.3% of the intensity calculated for this vibration has been transferred to the combination band at 2892 cm^{-1} in Ala-Nd_3 and 2893 cm^{-1} in Ala-$C^*d_1Nd_3$.

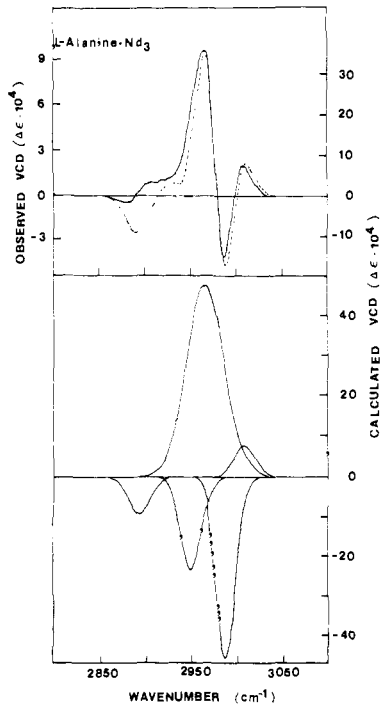

Figure 1. Spectral simulation (---) of the VCD spectrum of Ala-Nd_3 in the CH stretching region based on the intensities of LMO calculation II in Table I. The widths and frequencies of the Gaussian bands for the individual modes as shown below are based on spectral curve resolutions as described previously.[3] The experimental VCD spectrum (—) referred to a different intensity scale is overlayed for comparison.

C_{3v} patterns of (2, -1, -1) and (0, 1, -1) for the relative methyl CH stretches numbered as previously[3] ($C-H_{11}$, $C-H_{12}$, $C-H_{13}$). Choosing the other relative motions of the methyl CH stretches, i.e., (-1, 2, -1), (1, 0, -1) and (-1, -1, 2), (1-1, 0), gives the wrong sign pattern for both the FPC and LMO calculations. Thus, in calculation II we have the correct sign pattern for all eight CH stretching vibrations in these molecules, and we will focus our attention hereafter only on the results of this calculation.

If we compare the experimental rotational strengths with those of calculation II for all three molecules in Table I, we find that the theoretical values are larger than those observed for all bands except the band observed at 2987 cm^{-1} in alanine-C^*-d_1-N-d_3 which is calculated to be marginally less than experiment. The symmetric methyl vibration in alanine-N-d_3 is too large by the greatest factor, ~6, whereas all the remaining modes are too large by a factor of 3 or less. Nevertheless, even though the LMO results tend to be large by an average factor of 2 to 3, the relative intensities of the calculated and observed rotational strengths agree quite well, and, as mentioned above, all the calculated VCD signs agree with experiment. There is no large drop or major variation in the relation between calculated and observed rotational strengths upon CH deuteration as was observed in the FPC calculations of the previous paper. Thus, when the nuclear vibrational coupling between the methyl and methyne CH modes in alanine-N-d_3 is severed by deuteration, the LMO result in agreement with experiment shows a modest and not a drastic reduction in VCD intensity.

Considering next the dipole strength calculations, we find that the LMO results predict a reasonable set of relative intensities, but again the absolute value is too large by a factor of ~6. This factor is borne out quite consistently if the calculated dipole strengths are summed over the vibrations of the molecule and then compared with the corresponding experimental sum.

Finally, we list the anisotropy factor, g, which is simply $4R/D$. The overestimates of rotational and dipole strength as given by the LMO calculation tend to cancel in the ratio, but the experimental g values are larger than the calculated ones since the dipole strength was overestimated to a larger extent than the rotational strength.

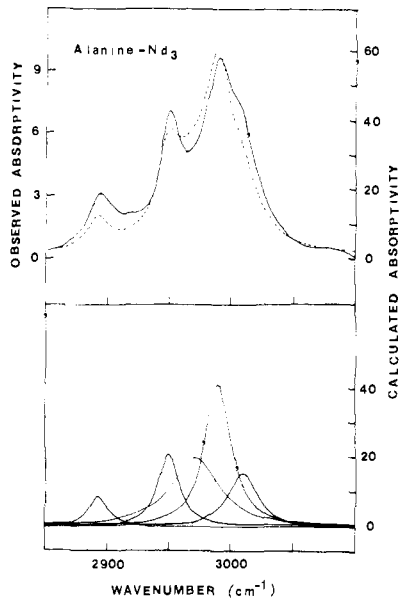

Figure 2. Comparison of experiment to theoretical simulation of the CH stretching absorption spectrum of Ala-Nd_3 based on the frequencies and intensities of calculation II in Table I and curve-resolved bandwidths as described previously.[3] Lorentzian band shapes were used.

Spectral Simulations

In Figure 1 we display the results of spectral simulations of the VCD spectrum of alanine-N-d_3 based on the LMO intensities from calculation II in Table I and the band positions and half-widths determined from the curve analysis described in the previous paper.[3] For comparison we have also plotted the experimental spectrum using a vertical scale which is approximately one-third of the theoretical scale in order to bring the two spectra into close proximity. In this view the excellent agreement between the LMO and observed relative VCD intensities can be clearly appreciated for the four fundamental vibrations. The two curves then deviate somewhat in the symmetric methyl stretching and overtone region between 2850 and 2950 cm^{-1}. This discrepancy could easily be due to *intrinsic* VCD intensity (positive) associated with the overtone bands of the methyl deformation modes which we do not account for in our calculations. Overtone and combination bands have been shown to have appreciable intrinsic strength,[12] and, further, hydrogen bending vibrations have exhibited very large VCD in the mid-infrared[13] in a number of cases including 3-methylcyclohexanone.[13] Owing to the rather low resolution (~8 cm^{-1}) of the VCD spectra, we found that Gaussian band shapes fit the observed spectra quite well, and the individual Gaussian bands used to obtain the simulated spectrum are shown in the lower portion of the figure.

The corresponding LMO simulation of the absorption spectrum of alanine-N-d_3 is shown in Figure 2. Since these FT-IR absorbance spectra, taken at 4-cm^{-1} resolution, closely approximate Lorentzian band shapes, we used Lorentzian bands to simulate the spectrum. The experimental absorbance spectrum is also shown using a scale which is roughly one-sixth the theoretical scale in keeping with the noted discrepancy in absolute intensity. The relative intensities are quite close, however. The individual Lorentzian bands are shown in the lower half of the figure.

Similar spectral simulations and comparisons of the LMO–VCD results to experiment for alanine-C^*-d_1-N-d_3 and alanine-C-d_3-N-d_3 are given in Figure 3. The same scales used in comparing the VCD curves for alanine-N-d_3 in Figure 1 are used here. As before Gaussian band shapes are also employed in these VCD

(12) Keiderling, T. A.; Stephens, P. J. *Chem. Phys. Lett.* **1976**, *41*, 46.
(13) Su, C. N.; Heintz, V. J.; Keiderling, T. A. *Chem. Phys. Lett.* **1980**, *73*, 157. Singh, R. D.; Keiderling, T. A. *J. Chem. Phys.* **1981**, *74*, 5347. Singh, R. D.; Keiderling, T. A. *J. Am. Chem. Soc.* **1981**, *103*, 2387. Heintz, V. J.; Keiderling, T. A. *Ibid* **1981**, *103*, 2395. Su, C. N.; Keiderling, T. A. *Chem. Phys. Lett.* **1981**, *77*, 494.

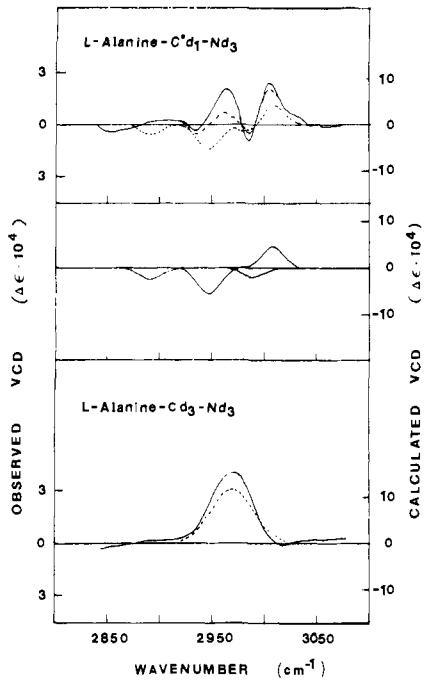

Figure 3. Comparison of experiment (—) to theory (---) for the CH stretching VCD spectra for Ala-$C^*d_1Nd_3$ and Ala-Cd_3Nd_3 using the methods described in Figure 1. The dash–dot VCD curve (—·—) represents the experimental VCD spectrum for Al-$C^*d_1Nd_3$ corrected for a ~10% impurity of Ala-Nd_3 as described in the text

simulations. There are two LMO–VCD simulation curves for alanine-C^*-d_1-N-d_3. The dashed curve is simply the composite of the individual components shown below it which are derived directly from the LMO–VCD intensities for these bands. The dashed–dot curve, which more closely follows the theoretical result, is obtained by subtracting 10% of the VCD spectrum for alanine-N-d_3 from the experimental VCD spectrum for alanine-C^*-d_1-N-d_3. The rationale for this mixture is the observed 10% impurity of alanine-d_0 in the Raman spectrum of alanine-C^*-d_1 reported in the first paper.[2] In the VCD spectrum of alanine-C-d_3-N-d_3 only one feature is observed and calculated. Agreement on the established relative scales is quite good, and no separate spectral representation of the component band is necessary.

Finally in Figures 4 and 5 we show the Lorentzian spectral simulations and comparison to the observed absorption spectra of alanine-C^*-d_1-N-d_3 and alanine-C-d_3-N-d_3. Very close spectral agreement results from the use of the 6:1 relative scales for observed vs. calculated intensities for alanine-C^*-d_1-N-d_3. The agreement is not as close for alanine-C-d_3-N-d_3, possibly because of the combination band at 3015 cm^{-1} which is also present in perdeuterioalanine in D_2O.[3]

Stereoprojections

Unlike FPC calculations of intensity which entail only nuclear motions, LMO intensity calculations are rich in the details of electronic displacements during vibration as well as the nuclear displacements. This additional information derives from the coupling of the motion of the centroids of LMOs with one another and with the nuclei. It is possible to display this electronic information in visual form by constructing molecular stereoprojections which show equilibrium and displaced positions for the nuclei and the LMO centroids for each vibration of interest. As we shall see, this can in turn lead to better understanding of the origin of LMO–VCD and absorption intensities.

The stereoprojections of the four fundamental CH stretching vibrations in alanine-N-d_3 are given in Figure 6 where the size of all displacements has been exaggerated for additional clarity. In the notation of the previous paper,[3] where the three hydrogens on the methyl group are labeled 11, 12, and 13, the mode pattern for the two antisymmetric stretches at 3009 and 2989 cm^{-1} is (0, 1, -1) and (2, -1, -1), respectively. We note that the unique CH

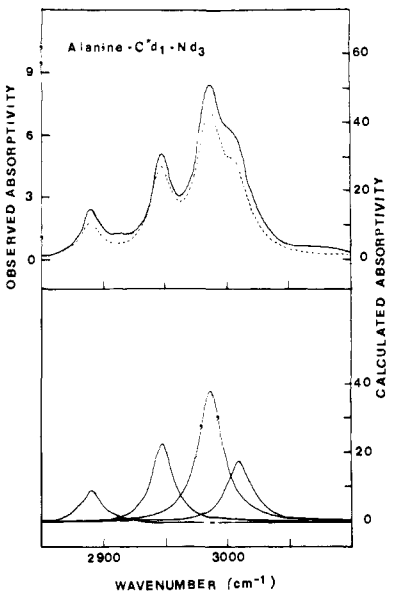

Figure 4. Comparison of experiment to the Lorentzian theoretical simulation for the CH stretching absorption spectrum of Ala-$C^*d_1Nd_3$ based on calculation II in Table I and the curve-resolved bandwidths.

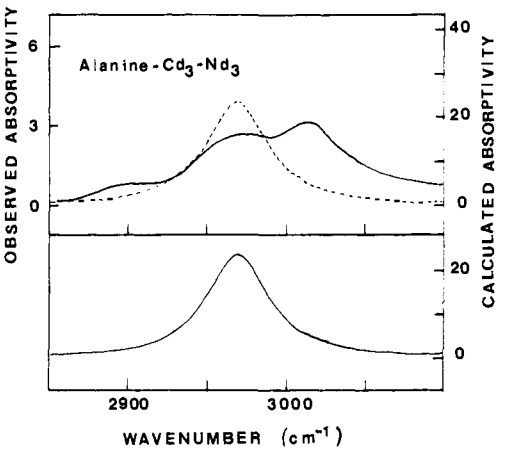

Figure 5. Comparison of experiment to the Lorentzian theoretical simulation for the CH stretching mode in Ald-Cd_3Nd_3 based on calculation II in Table I and the curve-resolved bandwidth.

methyl bond in the split methyl force field used for these calculations is the C–H(11) bond trans to the carboxylic acid group, which causes this bond to behave differently from the other two in these modes. The LMO centroids for this molecule lie on or very close to the bond axis for every bonding LMO in this molecule, and only the lone-pair LMOs attain other positions, as expected. LMO displacements in the methyl group closely follow the motions of the two nuclei with which they are associated, but, in addition, small but significant LMO displacements are calculated where nuclear displacements do not contribute.

Also in this figure we show the symmetric methyl and the methyne stretching modes. Strong mechanical coupling between the methyne stretching motion and the three methyl stretching motions is evident in all four vibrations. LMO displacements are particularly large throughout the molecule for the methyne stretch, involving even certain bonding LMOs in the carboxylic and amine groups which have virtually no nuclear motion. The richness of the LMO activity in this vibration clearly is related to the enormous VCD intensity of this mode (which is not predicted to be outstanding in the FPC–VCD calculations).

The stereoprojections of the corresponding four vibrations in alanine-C^*-d_1-N-d_3 and alanine-C-d_3-N-d_3 are shown in Figure 7. By noticing the LMO displacements in bonds which are not undergoing significant nuclear displacements, it is possible to appreciate how the LMO–VCD intensities for these modes are

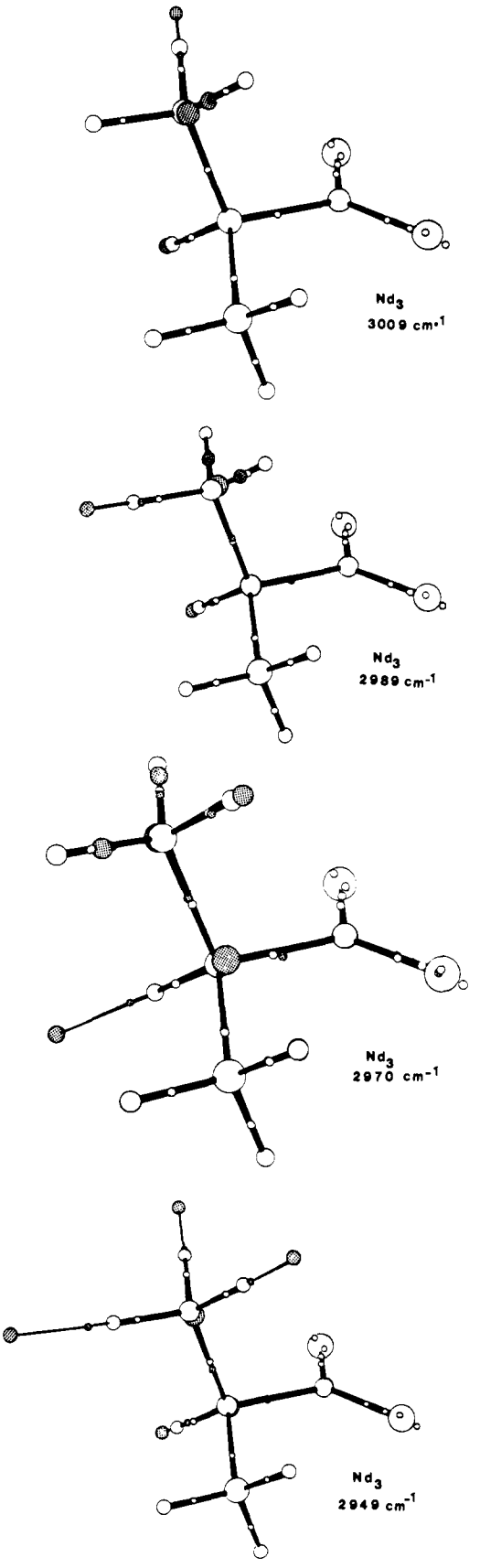

Figure 6. Stereoprojection showing the equilibrium positions of the nuclei (large white circles) and LMO centroids (small white circles) for Ala-Nd_3 and their exaggerated displacements (corresponding dotted circles) for all four CH stretching vibrations.

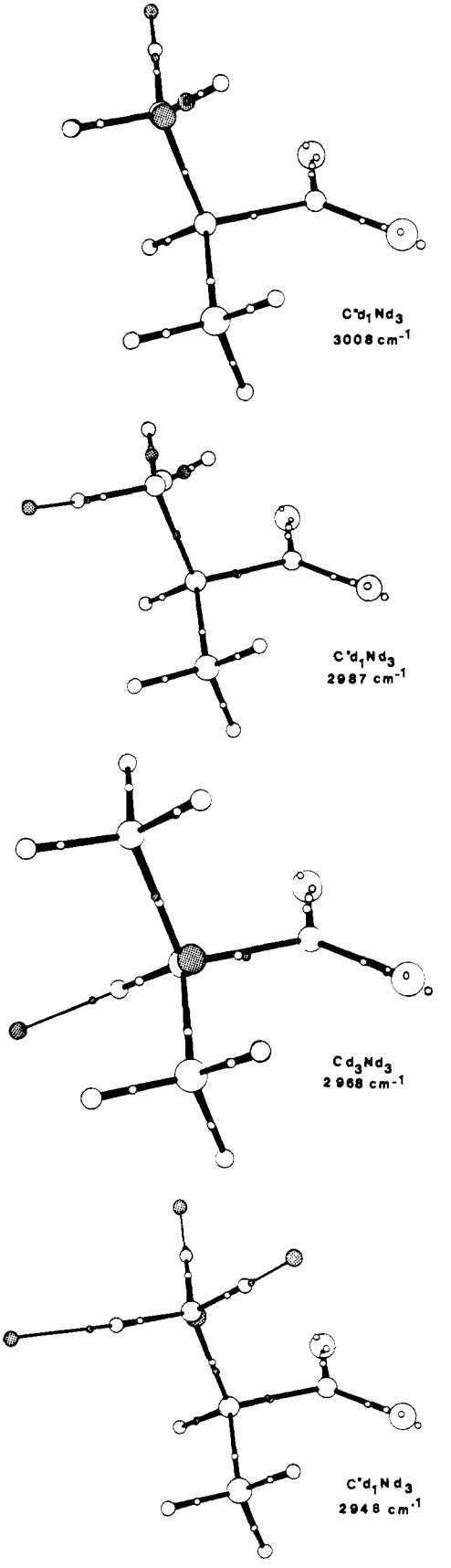

Figure 7. Stereoprojections of the four CH stretching vibrations in Ala-$C^*d_1Nd_3$ and Ala-Cd_3Nd_3. Equilibrium (white circles) and exaggerated displacements (dotted circles) for the nuclei (large) and the LMO centroids (small) are shown.

maintained at observed levels even though the coupling between the methyl and methyne nuclear displacements has disappeared from view.

The importance of LMO centroid displacements in nonvibrating regions of the molecule can be seen by considering eq 2 for the LMO rotational strength. For such a centroid displacement there

will be a set of terms from the orbital–orbital summation, coupling it to all other centroid displacements in the molecule. In some cases the separation vector $(\mathbf{r}_{k,0} - \mathbf{r}_{k',0})$ will be quite large. In addition there will be a similar set of nuclear-orbital terms which couple the centroid displacements to all the nuclear displacements, again with potentially large separation vectors. Thus displacements distributed throughout the molecule lead to expected large intensities such as those observed for the two methyne stretching modes.

Discussion of Absolute Intensities

From the preceding sections it is clear that the application of the LMO model to the calculation of VCD and absorption intensities using CNDO molecular orbital wave functions gives results which are in very close relative agreement with the observed spectra of the three alanine isotopomers for which we have data. We note that a single scale factor for all three VCD spectra and twice that scale factor for the three absorption spectra bring *all* the calculated and observed spectra into very close absolute agreement, as well. The agreement in relative intensities across these three molecules indicates that the LMO model is capable of providing a good description of the motion of electronic charge in local regions throughout these molecules and that this description is sufficient for predicting the VCD spectra. This can be contrasted with the results of the FPC calculations[3] where one scale factor cannot bring all the calculated VCD intensities into close agreement and where for alanine-*N*-d_3, the best case, the relative intensity comparison of FPC–VCD to experiment (Figure 6 of the previous paper) is not as favorable as the corresponding LMO–VCD comparison (Figure 1 of this work).

Because of the simplicity in the scaling relationship between the absolute strengths of the calculated (LMO) and observed VCD and absorption spectra, we believe that only one effect is responsible for the discrepancy. Furthermore, this effect appears to arise from the experimental conditions under which these spectra were obtained, namely, as aqueous solutions. In particular, we feel that water (D_2O) may effectively reduce the observed infrared VCD and absorption intensities via some unspecified mechanism which may have its origins in electrostatic screening or compensation. The evidence for this hypothesis can be found in the recent literature by inspection of ϵ_{max} values for various molecules that have similar CH bonds that are dissolved in aqueous solvent, on the one hand, and nonaqueous solvent, on the other. The comparison can in principle be made for ranges of $\Delta\epsilon$ values, but VCD spectra are more susceptible to cancellation and the details of local vibrational coupling than are the ordinary absorption spectra. As an example, if we compare the ϵ_{max} (at the antisymmetric stretching band frequency) values of alanine-*N*-d_3 and lactic-*O*-*d* acid-*O*-*d*[14] as D_2O solutions to α-phenylethylamine[15] in CCl_4, one finds $\epsilon_{max} \approx 10$ for both alanine and lactic acid and $\epsilon_{max} \approx 60$ for α-phenylethylamine; yet these three molecules each possess three methyl hydrogens and one methyne hydrogen (the phenyl CH stretches of α-phenylethylamine are higher in frequency by ~ 100 cm^{-1} and do not overlap). Another example is provided by the molecules alanine-*C*-d_3-*N*-d_3, tartaric-*O*-d_2-acid-*O*-d_2 in D_2O solution and 2,2,2-trifluoro-1-phenylethanol dissolved in CCl_4. The ϵ_{max} values for alanine and tartaric acid[16] are 3 to 4 and 6 per hydrogen, respectively, whereas the ϵ_{max} value for trifluorophenylethanol[15] is ~ 15.

In the examples discussed above, the molecules dissolved in D_2O are all acids, whereas the phenyl moiety appears in all molecules dissolved in CCl_4. Since it would be of interest to compare the absorption intensities of the *same* molecule dissolved in both CCl_4 and D_2O, we have carried out a preliminary set of measurements for alaninol [$NH_2C^*H(CH_3)CH_2OH$] where we find that ϵ_{max} near 2965 cm^{-1} is ~ 32 in D_2O and ~ 75 in CCl_4. While this change is not as large as those cited above, it does indicate clearly that absorption intensities can be significantly reduced merely by changing the solvent from CCl_4 to D_2O. While it is not unusual for hydrogen bonding to lead to a dramatic increases in the absorption strength[17] attended by band broadening and frequency shifts, the vibrational bands under consideration here are not affected in this way. They remain narrow in D_2O solution and their intensities *decrease* instead of increase in an environment where hydrogen bonding is otherwise promoted.

We have also investigated the possibility of systematic error in our CNDO–LMO program as a source of the discrepancy in absolute intensity, but have found none. Furthermore, using this same program, we have successfully calculated the LMO–VCD and absorption spectra of 3-methylcyclohexanone as a CCl_4 solution with the close agreement in absolute infrared (and VCD) intensity. Here 12 CH bonds give 12 CH stretching modes over a frequency range from 3000 to 2850 cm^{-1} having a ϵ_{max} near 120. The calculated LMO dipole strengths for these modes varied from roughly ~ 3 to 8.5×10^{-39} esu^2 cm^2 which is the same range, if not somewhat higher, than our six times overestimated dipole strengths in Table I which vary from ~ 1.5 to 5.7×10^{-39} esu^2 cm^2. This is further evidence that the CH stretching intensities for alanine in D_2O have unusually low values compared to other CH-bearing molecules dissolved in nonaqueous solution.

We next address the question of the discrepancy in the VCD absolute magnitudes between calculation and experiment. Most likely it arises from the same source as the infrared absorption discrepancy; however, it is not the same factor and reasons for this can be explored. First, it is possible that VCD is less susceptible to the general aqueous attenuation effect proposed above. For instance, if only the electric dipole transition moment is diminished by some factor, say 2 to 3, and not the magnetic dipole transition moment, then a factor of 4 to 9 attenuation will be observed for the dipole strength and only 2 to 3 for the rotational strength. Another possibility is that the intrinsic terms which describe VCD intensity arising from the rocking motion of LMOs about their centroids could account for this difference. This is unlikely for two reasons, the first being that estimates for the strength of this contribution[5,6] based on the dimensions and shapes of LMOs compared to molecular dimensions and shapes indicate that this contribution should be on the order of 10%. Second, two previous LMO–VCD calculations[6,7] have shown good agreement with observed rotational strengths, indicating that a major intensity contribution is not missing.

As a result of these considerations, it appears that solvent–molecule interactions lead to a reduction in the CH oscillator strengths in alanine by a mechanism which does not significantly alter the distribution, or vibrational redistribution, of electronic charge as described by our CNDO (LMO) calculations.

Summary and Conclusions

A number of rather specific statements and conclusions can be made as a result of these CNDO–LMO calculations. The method is very simple, yet appears to be sound for the calculation VCD intensities. The absorption intensities are simply the standard CNDO results and do not depend on approximations inherent in the LMO–VCD model. Once the geometry and nuclear vibrational displacements have been determined, the CNDO–LMO intensities have also been determined. There are no scaling factors or variable parameters which can obscure relationships between observed spectra and molecular structure and motion.

In this paper we have demonstrated the third successful application of the LMO model to VCD intensities. The present results are particularly significant since it is the first example of success with the LMO model where the FPC model clearly failed to account for sufficient VCD in most (6 of 8) of the modes.[3] In the process we have uncovered an interesting experimental pattern of absolute infrared absorption strengths for CH stretching modes

(14) Lal, B. B.; Nafie, L. A., unpublished results.
(15) Nafie, L. A.; Keiderling, T. A.; Stephens, P. J. *J. Am. Chem. Soc.* **1976**, *98*, 2715.
(16) Sugeta, H.; Marcott, C.; Faulkner, T. R.; Overend, J.; Moscowitz, A. *Chem. Phys. Lett.* **1976**, *40*, 397.
(17) Huggins, C. M.; Pimentel, G. C., *J. Chem. Phys.* **1955**, *23*, 896. Lord, R. C.; Nolin, D.; Stidham, H. D. *J. Am. Chem. Soc.* **1955**, *77*, 1365.

in molecules in aqueous solutions. We are thus led to conclude that our LMO–VCD and absorption intensities would be in closer absolute agreement if alanine were sampled in a nonaqueous solution.

Acknowledgment. Support for this research by grants from the National Science Foundation (CHE-8005227) and the National Institutes of Health (GM-23567) is acknowledged by L.A.N. One of us (P.L.P.) also acknowledges Dean D. L. Tuleen of Vanderbilt University for computing funds used to obtain the stereoprojections.

Registry No. Alanine-N-d_3, 19470-97-4; alanine-C^*-d_1-N-d_3, 27539-86-2; alanine-C-d_3-N-d_3, 73674-54-1.

Mass Spectrometry of Nucleic Acid Constituents. Electron Ionization Spectra of Selectively Labeled Adenines

Satinder K. Sethi, S. P. Gupta, E. E. Jenkins, C. W. Whitehead, Leroy B. Townsend, and James A. McCloskey*

Contribution from the Departments of Medicinal Chemistry and Biochemistry, University of Utah, Salt Lake City, Utah 84112. *Received October 8, 1981*

Abstract: The unimolecular decomposition of adenine following electron ionization has been studied on the basis of extensive isotopic substitution to establish the extent of site selectivity in fragment ion formation. Carbon-13 labeling at C-2, with earlier published work on [^{15}N]adenines, shows that elimination of HCN from the molecular ion is more than 90% derived from N-1 and C-2. Loss of NH_2 and NH_3 is predominantly from N-1, with complete retention of N-7 and N-9. $C_2H_4N_3^+$ (m/z 70) is formed by a rapid process with quantitative retention of N-1, C-2, N-3, C-4, and N-9. These results permit the assignment and estimation of ^{13}C and ^{15}N within the adenine nucleus, of potential value in studies of purine biosynthesis and metabolism. The adenine molecular ion is shown to be structurally identical with the m/z 135 fragment ion from adenosine on the basis of their collision-induced decomposition mass spectra. Equations are given for calculation of isotopic incorporation levels in fragment ions of adenine.

In recent years mass spectrometry has assumed an important role in the characterization of synthetic and natural nucleic acid bases and nucleosides.[1] In terms of systematic examination of detailed fragmentation processes, as opposed to largely descriptive reports of spectra, the greatest effort has been expended on nucleosides rather than the corresponding bases.[1-3] This has been due largely to the greater difficulty of introduction of isotopic labels into selected positions of the heterocyclic nucleus and to the inherently complex nature of heteroaromatic decomposition processes,[4,5] which further strengthens the need for selectively labeled models. In addition to purposes of structural characterization, study of the unimolecular decomposition processes of purines and pyrimidines serves to further expand the knowledge of the behavior of polynitrogen heterocycles, an area of gaseous ion chemistry that has received generally superficial attention with respect to mechanistic details. In the case of purines such as adenine and guanine, the establishment of site selectivity in the formation of fragment ions is of potential value for the mass spectrometric location of stable isotopes in the purine nucleus, in studies of purine biosynthesis and metabolism.[6]

The mass spectrum of adenine was first reported by Shannon and Letham,[7] and independently by Rice and Dudek,[8] both of whom outlined the principal ionic decomposition routes. In subsequent work, Occolowitz[9] studied the sequential expulsion of two HCN molecules using [8-^{14}C]adenine and N-deuterated adenines, while Leonard and Henderson examined the same reaction series on the basis of ^{15}N labels in two positions[10] and later in each of the five possible positions.[11] The inclusion of N-1 in the first loss of HCN was demonstrated by ^{15}N labeling,[11] contrary to expectations resulting from ^{2}H- and ^{14}C-labeled adenines.[9]

We have studied the fragmentation processes of adenine on the basis of its high-resolution mass spectrum, on decomposition pathways established by metastable ion measurements, and on extensive isotopic substitution. The five isomeric ^{15}N-labeled adenines have been synthesized and examined, along with [2-^{13}C]-, [8-^{14}C]-, [2-^{2}H]-, and [8-^{2}H]adenine, to establish the extent of positional selectivity in the formation of five sets of fragment ions that have not previously been examined.

Experimental Section

General Remarks. [^{15}N]Ammonia (several lots, >99 atom %) used in syntheses was purchased from Mound Laboratories, Miamisburg, OH. [2-^{13}C]Adenine was obtained from Merck Isotopes, St. Louis, MO, and [8-^{14}C]adenine from I.C.N., City of Industry, CA. [2-^{2}H]Adenine was prepared by back exchange of D-8 (100 °C, 1 h) in [2,8-$^{2}H_2$]adenine, which had earlier been prepared by a catalytic exchange procedure.[12]

Starting materials for the [^{15}N]adenines were prepared by literature procedures; however, the reaction conditions reported in the following sections commence with the first introduction of the ^{15}N isotope. An authentic unlabeled sample of each compound was used for direct TLC comparison to corroborate structural assignments of the labeled adenines and of all intermediates. Ultraviolet spectra were recorded with a Beckman Acta C III spectrophotometer and infrared spectra were recorded on a Beckman IR 100 spectrophotometer. Melting points were determined with a Thomas-Hoover capillary apparatus and are uncorrected.

[**1**-^{15}N]**Adenine (3).** A mixture of 4(5)-amino-5(4)-cyanoimidazole[13] (**1**, 48 mg) and diethoxymethyl acetate[14] (DEMA, 3.5 mL) was stirred

(1) Hignite, C. In "Biochemical Applications of Mass Spectrometry"; Waller, G. R., Dermer, O. C., Ed.; Wiley-Interscience: New York, 1980; pp 527–566.
(2) Hignite, C. In "Biochemical Applications of Mass Spectrometry"; Waller, G. R., Ed.; Wiley-Interscience: New York, 1972; pp 429–447.
(3) McCloskey, J. A. In "Basic Principles in Nucleic Acid Chemistry", Ts'o, P. O. P., Ed.; Academic Press: New York, 1974; Vol. I, pp 209–309.
(4) Budzikiewicz, H.; Djerassi, C.; Williams, D. H. "Mass Spectrometry of Organic Compounds"; Holden-Day: San Francisco, 1967; pp 582–595.
(5) Porter, Q. N.; Baldas, J. "Mass Spectrometry of Heterocyclic Compounds"; Wiley-Interscience: New York, 1971.
(6) *Adv. Exp. Med. Biol.* **1980**, *122B*, 1–86.
(7) Shannon, J. S.; Letham, D. S. *N. Z. J. Sci.* **1966**, *9*, 833–842.
(8) Rice, J. M.; Dudek, G. O. *J. Am. Chem. Soc.* **1967**, *89*, 2719–2725.
(9) Occolowitz, J. L. *Chem. Commun.* **1968**, 1226–1227.
(10) Leonard, N. J.; Henderson, T. R. *J. Am. Chem. Soc.* **1975**, *97*, 4990–4999.
(11) Barrio, M. C. G.; Scopes, D. I. C.; Holtwick, J. B.; Leonard, N. J. *Proc. Natl. Acad. Sci. U.S.A.* **1981**, *78*, 3986–3988.
(12) Kinoshita, T.; Schram, K. H.; McCloskey, J. A. *J. Labelled Compd. Radiopharm.*, in press.
(13) Ferris, J. P.; Orgel, L. E. *J. Am. Chem. Soc.* **1966**, *88*, 3829–3831.

0002-7863/82/1504-3349$01.25/0